

## PHOTOELASTIC SOLUTION OF STRESSES IN THE ELASTIC FOUNDATION SUPPORTING A PLATE

A. J. DURELLI†, V. J. PARKS‡ and J. S. NORGARD§

Civil and Mechanical Engineering Department, The Catholic University of America, Washington, D.C.

**Abstract**—The stress distribution in a continuous, linear elastic foundation supporting a centrally loaded circular plate has been analyzed using the photoelastic freezing method. At the interface between plate and foundation the axial displacements and the radius of the contact surface were also determined. Comparisons are made with theoretical solutions. The particular combination of epoxies used in this analysis makes the photoelastic method easily applicable to the solution of many foundation problems.

### INTRODUCTION

THE analysis of stresses in foundations is often conducted with the assumption of independent linear spring behavior of the foundation material as suggested by Winkler [1]. A thorough and systematic study of the two-dimensional problem based on this assumption has been presented by Hetenyi [2]. Considerations on theoretical three-dimensional solutions based on Winkler's assumption and on continuous behavior can be found in Timoshenko and Woinowsky-Krieger [3]. Laermann [4] has solved the differential equations for plates on elastic foundations with creep and gives values for the case with a ring load on the plate.

Two of the authors of this paper have experimentally solved the problem of the beam on an elastic foundation, modeling the foundation as a linear continuous media and using two-dimensional photoelasticity and rubber models [5].

In this paper an experimental solution of the three-dimensional stress distribution in a foundation is presented. The foundation is supporting a circular plate, which is subjected to a load acting at its center, in the direction perpendicular to the plane of the plate. The photoelastic freezing technique, as described in [6], has been used for this three-dimensional analysis. The geometry of the model is considered an approximation of an infinite plate resting on a semi-infinite elastic foundation.

### PHOTOELASTICITY TEST

#### *Models*

The material used for the foundation model was an epoxy compound manufactured using a formula suggested by Sampson [7]. The critical temperature of this material is

† Professor.

‡ Associate Professor.

§ Post-Doctoral Fellow, presently at Technical University of Denmark, Lyngby, Denmark.

about 60°C. After casting the foundation model, which was made cylindrical in shape, the top and bottom surfaces were machined.

The model of the plate was made of another epoxy resin, Hysol 4290, and machined on all surfaces. The critical temperature of this material is 120°C. The test temperature was 73°C, so that the plate material is in the glassy state when the foundation material is in the rubbery state. This simulates the usual condition of a hard plate and a soft foundation.

Figure 1 shows the geometry of the plate and the foundation. The diameter of the cylindrical foundation is  $2r' = 4.86$  in. and the height is about 7.33 in. The thickness,  $h = 0.180$  in. of the plate was determined by a desire to limit the radius of the contact area between the plate and the foundation to about half of the total radius of the two parts. The estimate was based on a paper by Weitsman [8]. The center axis in the cylindrical coordinate system used is the  $z$ -axis and the radial axis is  $r$ , as shown in Fig. 1. They were both normalized with the contact radius,  $r_c$ . The tangential coordinate is  $\theta$ .

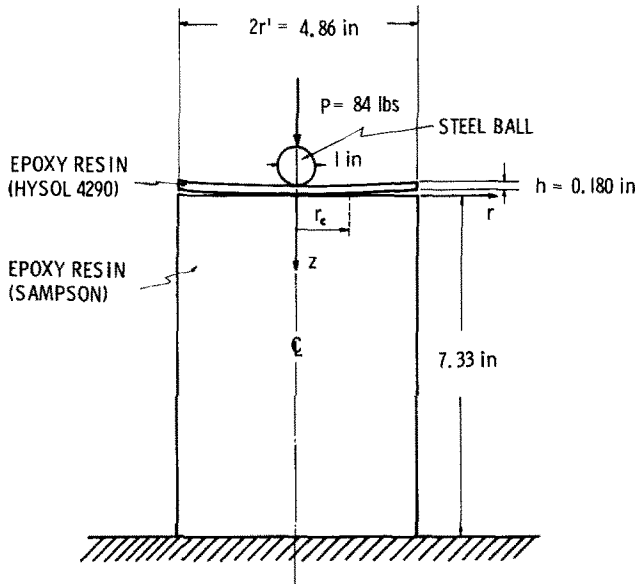


FIG. 1. Geometry and loading for photoelastic test.

#### *Loading, freezing and calibration*

The load  $P$  was applied vertically to the center of the plate by a steel ball, 1 in. in diameter, as shown in Fig. 1.

A low level of friction is not uncommon in practice. In the modeling it has added importance since the thermal changes might produce unwanted stresses in the bodies. If it is desired to model a plate and foundation with high friction, then the coefficient of thermal expansion of the model materials should be matched to avoid thermal stresses. This was done in other problems [9].

A ring and a disk from the foundation material and a ring from the plate material were loaded diametrically for the determination of the mechanical and optical constants. The loaded model and the loaded rings and disk were placed in an oven.

The temperature was raised at a rate of  $1^{\circ}\text{C/hr}$  to  $73^{\circ}\text{C}$  and lowered at a rate of  $0.5^{\circ}\text{C/hr}$  to room temperature. After completing the temperature cycle, which lasted about a week, the loads were removed.

From the calibrating rings and disk the freezing stress fringe value for the Sampson compound used for the foundation was found to be  $f = 0.675 \text{ lb/in. fringe}$ , its modulus of elasticity  $E_f = 1520 \text{ psi}$  and Poisson's ratio estimated to  $\nu_f = 0.49$ . For the plate material, Hysol 4290, the modulus of elasticity obtained at the high temperature was  $E_p = 255,000 \text{ psi}$  and Poisson's ratio was estimated to  $\nu_p = 0.37$ .

### Slicing and Photographing

Figure 2 shows how 5 slices were removed from the frozen foundation model. The slices were cut with a band saw and precaution was taken to limit heating, which could cause annealing in this epoxy because of its low critical temperature. Annealing tends to reduce the fringe order. After cutting, the slices were sanded and immersed in oil for photographing and determination of fractional fringe order. Figure 3 shows dark and light field isochromatics of the meridian slice. As expected the isochromatic pattern of transverse slices show axial symmetry. Isoclinics were also recorded and from them isostatics were determined. These are shown in Fig. 4 for the meridian slice.

## ANALYSIS

### Radial and circumferential stresses in the foundation

The shear stresses  $\tau_{rz}$  in the foundation can be obtained from the isochromatics and isostatics of the meridian slice, No. 1. The equation to be used is [6]

$$\tau_{rz} = -n \frac{f}{t} \sin 2\theta \quad (1)$$

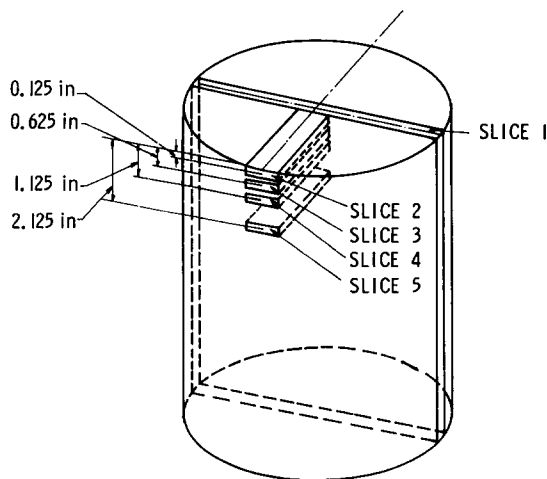


FIG. 2. Slicing plan for "frozen" foundation.

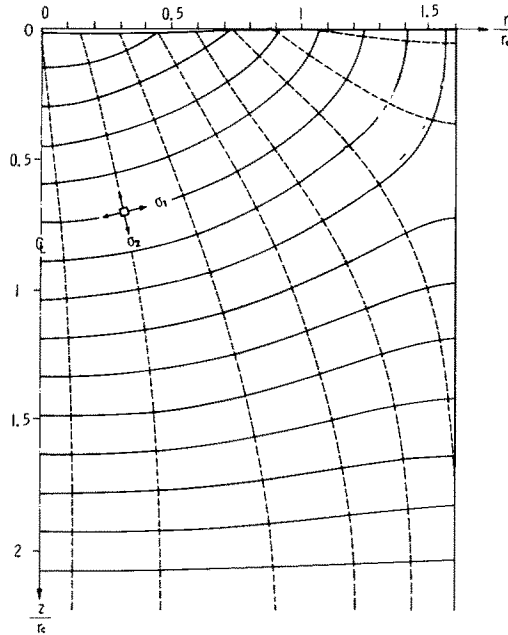


FIG. 4. Isostatics for the meridian slice of an elastic foundation supporting a plate.

where  $n$  is the fringe order at the considered position,  $t$  is the thickness of the slice,  $f$  is the stress fringe value for the material used and  $\theta$  is the angle measured from the  $r$ -axis counter-clockwise to the direction of the principal stress.

From transverse slices such as 2, 3, 4 and 5 the secondary principal stress difference can be obtained using the following equation

$$\sigma_r - \sigma_\theta = 2n \frac{f}{t}. \tag{2}$$

Assuming that there are no body forces, the differential equation of equilibrium for the axisymmetric case can be expressed in cylindrical coordinates as [10]:

$$\frac{\partial \sigma_r}{\partial r} + \frac{\partial \tau_{rz}}{\partial z} + \frac{\sigma_r - \sigma_\theta}{r} = 0. \tag{3}$$

In finite difference form, this equation can be written as

$$\sigma_r = \sigma'_r - \sum_{r=r'}^r \left[ \frac{\Delta r_{rz}}{\Delta z} \Delta r + \frac{\sigma_r - \sigma_\theta}{r} \Delta r \right], \tag{4}$$

where  $\sigma'_r$  is a known value of  $\sigma_r$  at a certain point, in this case at the vertical surface of the foundation, where  $\sigma_r = 0$ .  $\Delta \tau_{rz}$  is the change in shear stress  $\tau_{rz}$ , in the interval  $\Delta z$  in vertical direction and is obtained from equation (1). The value of  $\sigma_r - \sigma_\theta$  is given by (2).

The radial stresses were computed from equation (4) by numerical integration at four levels of  $z$ . The circumferential stresses were then obtained from equation (2).

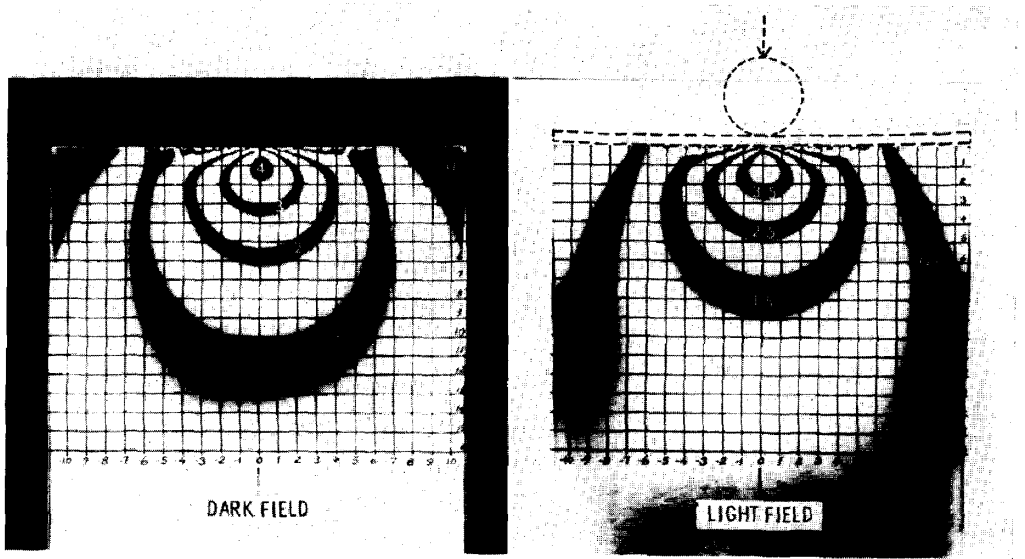


FIG. 3. Isochromatics in the meridian slice of an elastic foundation supporting a plate.

### Vertical stresses in the foundation

Knowing  $\sigma_r$ , the vertical stresses  $\sigma_z$  can be obtained from the photoelastic measurements, using the following equation [6]:

$$\sigma_z = \sigma_r - 2n \frac{f}{t} \cos 2\theta \quad (5)$$

where  $n$  is the fringe order in the meridian slice and  $\theta$  is the angle of the principal stress.

### Pressure at interface

The contact pressure at the interface between plate and foundation can be obtained also by numerical integration using a second equation of equilibrium [10]:

$$\sigma_z = \sigma'_z - \sum_{z=z'}^z \left[ \frac{\Delta \tau_{rz}}{\Delta r} \Delta z + \frac{\tau_{rz}}{r} \Delta z \right], \quad (6)$$

where  $\sigma'_z$  is the known value of  $\sigma_z$  at the starting point,  $z'$ .

The integration up to the interface has been carried out starting from three horizontal levels and over the entire  $r$ -range.

### Corrections

The above mentioned equations assume that the photoelastic values,  $n$  and  $\theta$  in the meridian slice correspond to a plane through the centerline of the foundation. However, the slice from which those values were obtained had a thickness  $t$  and the measured fringe orders and angles correspond to averages over this thickness. The errors introduced were largest for small values of  $r$  and some corrections were made to eliminate the errors.

## RESULTS

The isochromatic patterns of the meridian slice are shown in Fig. 3. No pattern appeared in slices 2–5 because the maximum fringe order was 0.8 and a compensation technique was used.

In Fig. 4 the isostatics for slice 1 are presented. If there were no friction between plate and foundation there would be no shear stresses and the isostatics would meet the top surface perpendicularly. This is not the case in Fig. 4 and in Fig. 9 the shear stresses  $\tau_{rz}$  at the top surface are plotted. Those shear stresses were obtained from equation (1). The direction of the principal stresses in slices 2–5 is radial and tangential because of axial symmetry.

The values of  $\sigma_z$ ,  $\sigma_r$ , and  $\sigma_\theta$ , obtained by numerical integration are plotted in Figs. 5–7 for different horizontal levels. For  $\sigma_r$  and  $\sigma_\theta$  only 3 curves are shown because the values corresponding to  $z/r_c = 1.258$  were very small and about the same as those corresponding to  $z/r_c = 0.667$ .

The displacement of the top surface of the foundation was measured on the “frozen” slice No. 1 and plotted in Fig. 8. The displacement at  $r = r_c$  was chosen to be zero. For  $r \leq r_c$  the displacement of the plate coincides with the displacement of the foundation, but for  $r > r_c$  both are different.

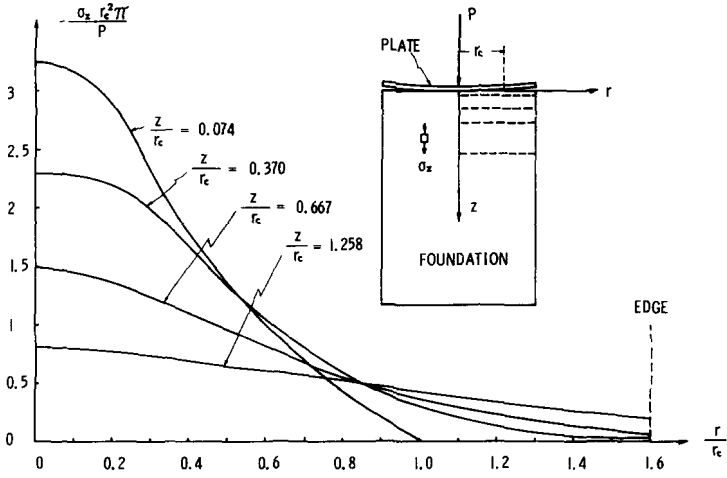


FIG. 5. Vertical stresses,  $\sigma_z$  at four levels in elastic foundation supporting a plate.

The interface pressure  $p = -\sigma_z$  between the plate and the foundation is plotted in Fig. 9 and compared with two theoretical solutions. From the experimental results the value of the radius of the contact surface  $r_c$ , was determined. This value was used as a characteristic length for normalizing the coordinates and the stresses in all plots.

### COMPARISON WITH THEORIES

#### Contact radius

As mentioned above Weitsman [8] has given the expression to determine the theoretical radius  $r_{c,t}$  of the circular area of contact between plate and foundation. Assuming an

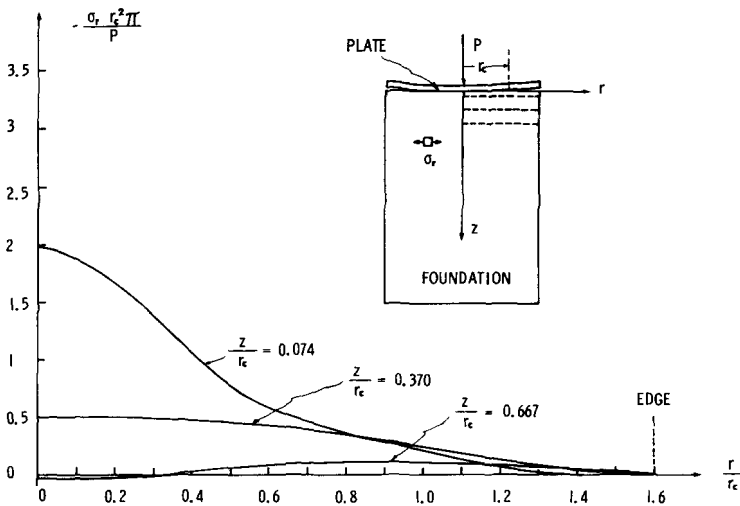


FIG. 6. Radial stresses,  $\sigma_r$  at the three levels in elastic foundation supporting a plate.

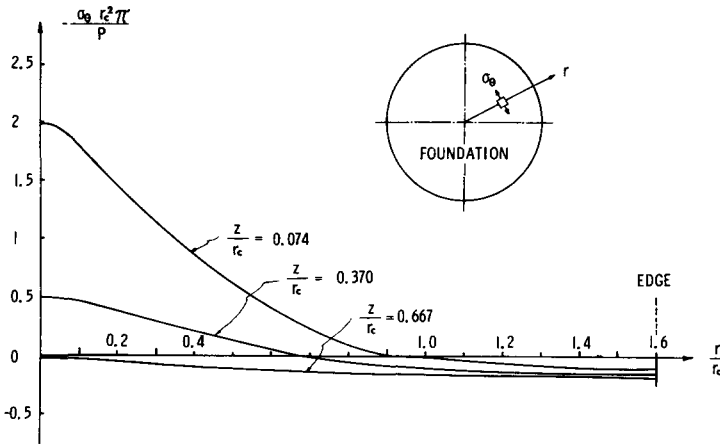


FIG. 7. Tangential stresses,  $\sigma_\theta$  at three levels in elastic foundation supporting a plate.

infinite plate, a semi-infinite elastic foundation and no friction at the interface, Weitsman's theory gives

$$r_{c,t} = 1.61h^{-3} \sqrt{\left[ \frac{(1-\nu_f^2)E_p}{(1-\nu_p^2)E_f} \right]} \tag{7}$$

In the present case equation (7) gives

$$r_{c,t} = 1.53 \text{ in.}$$

Weitsman's theory was revised by Pu and Hussain [11]. The revised theory gives

$$r_{c,t} = 1.74 \text{ in.}$$

Yoon and Rim [12] have analyzed the problem, using a computer. For the present case their program gives

$$r_{c,t} = 1.60 \text{ in.}$$

The contact radius measured on the photoelastic model was

$$r_c = 1.69 \text{ in.}$$

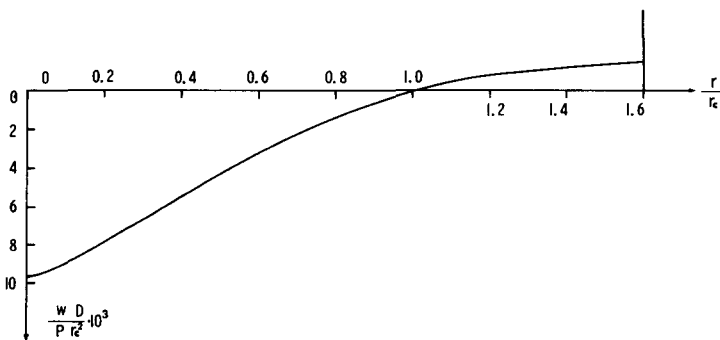


FIG. 8. Displacement,  $w$  at the top surface of an elastic foundation supporting a plate.



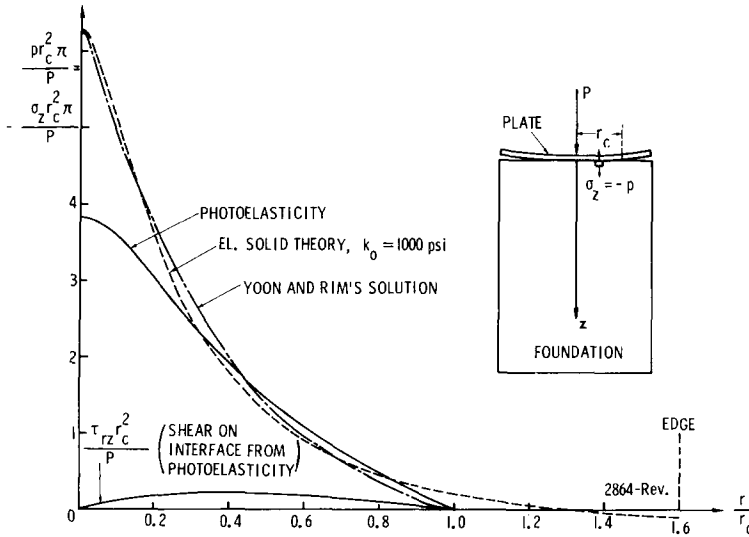


FIG. 9. The interface pressure and shear stresses between an elastic foundation and a loaded plate.

*Theories for interface pressure*

All theoretical solutions of problems similar to the one studied here make three assumptions which do not agree well with the experimental conditions, namely (1) no friction between plate and foundation, (2) infinite size of plate and (3) the load applied at a point.

Two theoretical solutions can be found in Timoshenko and Woinowsky-Krieger's book [3]. One of these solutions is based on Winkler's assumption that the reaction pressure from a foundation at any point is proportional to the displacement of the foundation at the point, i.e.  $p = kw$ , where  $k$  is called modulus of the foundation [2]. The value of  $k$  for the present foundation has not been determined and no comparison between the experiment and Winkler's theory is shown.

*Elastic solid theory of interface pressure*

In the other theoretical solution, the foundation is considered as an elastic solid. Besides the three above mentioned assumptions it is further assumed that there is contact between plate and foundation in zones of negative pressure.

The elastic properties of the foundation in this theory are characterized by

$$k_0 = \frac{E_f}{2(1 - \nu_f^2)} \tag{8}$$

For the material used in the test, the value is

$$k_0 = 1000 \text{ psi.}$$

The curve for the interface pressure based on this experimental  $k_0$  value is shown in Fig. 9.

*Yoon and Rim's solution*

Weitsman [8] has also developed a theory for the interface pressure based on the three above mentioned assumptions but assuming no contact when pressure goes below zero. The theory was improved by Pu and Hussain [11] and it was used to compute the radius of contact for the test data of this paper.

Based on the same assumptions Yoon and Rim have developed a computer program [12]. Applied to the data used in the photoelastic experiment, the program gives the distribution shown in Fig. 9. The results have been obtained by courtesy of Professor K. Rim.

**ACCURACY**

Appreciable errors may accumulate in the numerical integration procedure. Some computations have been made of the standard deviations of the stresses  $\sigma_z$ ,  $\sigma_r$ ,  $\sigma_\theta$ , based on estimates of the random errors of each of the directly measured quantities. For the three stress components the standard deviations are almost the same and highest near the center line. For  $z/r_c = 0.074$  the normalized values of  $\sigma_z$ ,  $\sigma_r$ , and  $\sigma_\theta$  3.3, 2.0 and 2.0, respectively at the centerline, and their standard deviation is 0.2. For  $z/r_c = 0.370$  the corresponding stress values are 2.3, 0.5, and 0.5 and their standard deviation is 0.1.

The systematic error from using equation (4) as an approximation to equation (3), is estimated to be negligible compared with the standard deviation. The corrections mentioned above to account for the finite thickness of the slices are carried on up to  $r$  values where the errors due to thickness of the slice are negligible. 0.1.

For all four  $z$  levels in Fig. 5 a check for the  $\sigma_z$  values has been made by integrating  $\sigma_z$  over the circular, horizontal plane. The integrated values were found to be in agreement with the total load on the plate within the random error. The relative deviations of the integrated values from the total load for  $z/r_c = 0.074, 0.370$ , etc. are  $-6, +10, +1$  and  $+2$  per cent, respectively.

The interface pressure, Fig. 9, is obtained as an average of integrated values from  $\sigma_z$  at 3 horizontal levels. Near the centerline  $p\pi r_c^2/P = 3.8$  and the standard deviation is about 0.2.

**CONCLUSIONS**

The horizontal distributions of the stresses in the foundation are rapidly equalized with increasing depth,  $z$ , see Figs. 5–7. The maximum stress is the vertical stress at the interface where

$$\sigma_{z,\max} = 3.8 \frac{P}{r_c^2 \pi},$$

see Fig. 9.

Neither of the theoretical solutions shown in Fig. 9 seems to be in very good agreement with the experiment, probably mainly due to the assumption of a point load in the theories. The three theoretically obtained values of the radius of contact are in very good agreement with the experimental one, in spite of the fact that the assumptions for the theory about infinite plate, point load and no friction are not completely satisfied.

*Acknowledgments*—The research program was supported by the National Science Foundation. The authors would like to express their gratitude to the Foundation and their thanks to Dr. M. Gaus for his continuous understanding and encouragement. The authors also thank Prof. K. Rim for applying his computer program to our problem. Also thanks to C. Y. Kim for the drawing of the figures and Mrs. D. Hunt for the typing. The casting of the foundation was done by H. Miller.

## REFERENCES

- [1] E. WINKLER, *Die Lehre von der Elastizität und Festigkeit*, p. 182. Prag. Dominicus (1867).
- [2] M. HETENYI, *Beams on Elastic Foundation*. University of Michigan Press (1946).
- [3] S. TIMOSHENKO and S. WOINOWSKY-KRIEGER, *Theory of Plates and Shells*, chapter 8. McGraw-Hill (1959).
- [4] K. H. LAERMANN, Der Einfluss des Kriechens auf die Sohlpressungen unter elastisch gebetteten Konstruktionen. *Forsch. Ing.-wes.* **36**, 85–89 (1970).
- [5] A. J. DURELLI, V. J. PARKS, CARSON K. C. MOK and HAN-CHOW LEE, Photoelastic study of beams on elastic foundations. *J. Struct. Div. Am. Soc. Civ. Engrs* 1713–25 (1969).
- [6] A. J. DURELLI and W. F. RILEY, *Introduction to Photomechanics*, Prentice-Hall (1965).
- [7] R. S. SAMPSON, A three-dimensional photoelastic method of analysis of differential contraction stresses. *Exp. Mech.* **3**, 225–237 (1963).
- [8] Y. WEITSMAN, On the unbonded contact between plates and an elastic half space. *J. appl. Mech.* **36**, 198–202 (1969).
- [9] A. J. DURELLI, V. J. PARKS, H. C. FENG and F. CHIANG, Strains and Stresses in Matrices with Inserts, Mechanics of Composite Materials, *Proc. Fifth Symp. on Naval Str. Mechanics*, edited by F. W. WENDT, H. LIEBOWITZ and N. PERRONE, pp. 265–336, Pergamon (1970).
- [10] S. TIMOSHENKO and J. N. GOODIER, *Theory of Elasticity*, p. 343. McGraw-Hill (1951).
- [11] S. L. PU and M. A. HUSSAIN, Note on the unbonded contact between plates and elastic half space. *J. appl. Mech.* **37**, 859–861 (1970).
- [12] K. E. YOON and KWAN RIM, Analysis of unbonded contact problems through application of an optimization technique. *Dev. Mech.* **6**, 659–672.

(Received 1 June 1971; revised 31 March 1972)

**Абстракт**—Путем использования фотоупругого метода заморживания, исследуется распределение напряжений в непрерывном линейно-упругом фундаменте, несущим центрально нагруженную круглую пластинку. Определяются, также, осевые перемещения и радиус поверхности контакта, на поверхности раздела между пластинкой и фундаментом. Даются сравнения с теоретическими решениями. Частный состав эпоксидов использованный в этом анализе, делает фотоупругий метод легко приложенным к решению большинства задач фундаментов.